

Ecological Land Conservation Strategies Explained By Urban Growth and Climate Change

Shi Zhao

Beijing University of Civil Engineering and Architecture

Quan Shao (✉ shaoquan@bucea.edu.cn)

Beijing University of Civil Engineering and Architecture

Research Article

Keywords: Ecological land conservation, Urban growth, Climate change, Risk scenarios

Posted Date: February 25th, 2021

DOI: <https://doi.org/10.21203/rs.3.rs-230596/v1>

License: © ⓘ This work is licensed under a Creative Commons Attribution 4.0 International License.

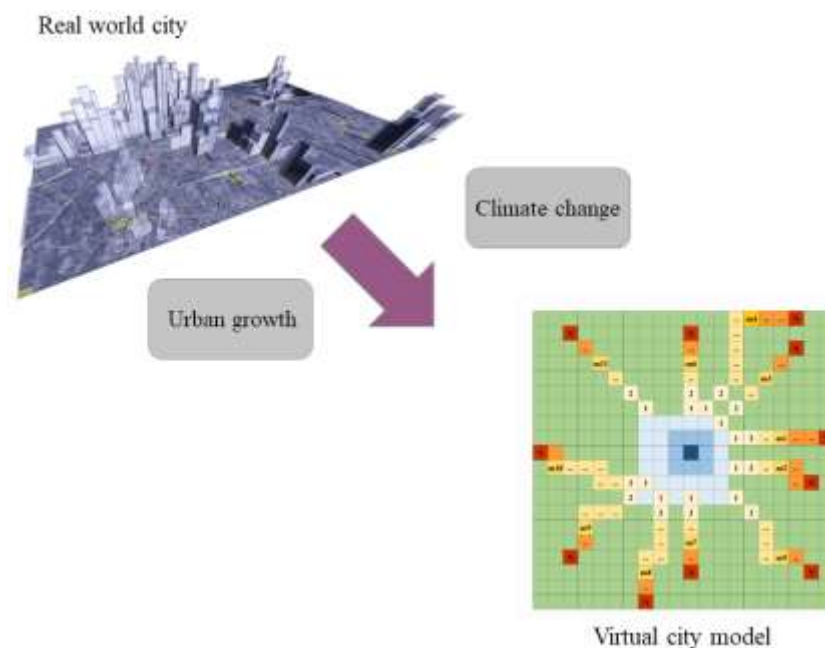
[Read Full License](#)

Ecological land conservation strategies explained by urban growth and climate change

Shi Zhao, Quan Shao*

School of Urban Economics and Management, Beijing University of Civil Engineering and Architecture, Beijing, China

Graphical abstract:



Abstract

Rising urban population throughout the world have boosted land use demand, intensifying pressure of ecological land resources linked with climate change. By incorporating risk into assessment, people can discourage excessive growth in megacity areas. Here, we propose a generalized analysis framework of ecological land conservation by devising a public goods game, which simultaneously considers population gravity and climate change along with interactions. Our method describes strategic conservation under the growth risk of urban

* Corresponding author.

email: shaoquan@bucea.edu.cn

boundary, where recurs across multiple rounds. We find that a compact and reasonable city with spatial structure will reduce erosion risk of ecological land and the lower costs of conservation, and higher its benefits. The conservation costs at the equilibrium do not increase with the degree of emphasis on the future, which show threshold effect. Ecological lands at the city boundaries have highest eroding risk, but rather pay a disproportionate amount of cost in this asymmetric game environment, which makes controlling erosion of ecological land less sustainable. Overall, our results suggest that implementing conservation strategies will efficiently reduce aggregate damages of urban growth and mitigate climate change, otherwise it may increase ecological land damages substantially.

Keywords

Ecological land conservation; Urban growth; Climate change; Risk scenarios

Introduction

Global urban areas are expanding with population dynamics, exerting adverse impact on ecological land seriously, this land erosion change is considered the emergence closely linked to dual challenges of urban growth and climate change^{1,2,3}. The trend on large-scale demographic migration across the world from rural to urban areas is unequivocal over the next decades. A huge number of populations will continue migrating to form a serious of mega-cities, and 68% of global population is projected to reside in urban areas by 2050⁴. In particularly, East Asian, Southeast Asian, and African areas, which estimates rapid urban growth will result in more than 80% of ecological land loss in urban fringe^{5,6}. The impacts of these changes may be considerable^{7,8,9,10,11}. Mega-cities requiring more population to be accommodated, increasing of urban built-up area reduces of the magnitude on ecological land. This morphology of urban change is responsible for more 70% of CO₂ emissions, consuming approximately 67-76% of global energy¹². Because of that, dramatic degradation of ecological land drives furtherly global warming¹³.

Another key insight is the climate response to spatial attraction changes for cities is that

heat island effect¹⁴, which are further exacerbated various direct or indirect extra heat damages for urban dwellers' job, living, and their health^{15,16,17}. Prior research shows that the urban-rural temperature difference can reach more than 10 °C across a mega-city areas affected by population and land, individual city exhibit different reactions to extreme cold and heat under climate change¹⁸. Therefore, the spatial pattern of ecological land in urban area also directly shapes the situation when dwellers facing climatic stress¹⁹.

The erosion process of ecological land (this study refers to forest, grassland, wetland, and waters are ecological land types) is the short-term or long-term result of the interaction and complex influences of the economic activities, population migration, environmental policies, and urban planning²⁰. Recent research has shown that global competition patterns for developing ecological land between urban multiple uses has led to a dramatic loss of ecosystem services, and the negative impacts on alleviation and adaptation of climate change^{21,22}. For example, decreasing of ecological land has estimated that global species richness and abundance were 4.2% and 2% lower from 1982 to 2015²³. Moreover, forestry erosion process caused by urban growth has exacerbated global GHGs²⁴. Historical evidence and future projections suggest that most cities are likely to suffer more natural and economic losses from erosion of ecological land²⁵.

In the context of urban growth and climate change, as one of the most irreversible natural resources, degradation process of ecological land is likely greater uncertainty in the future²⁶. Efforts to apply various simulation and empirical approaches to explicitly describe process of ecological land erosion caused by urban growth usually have included the partial least squares method^{27,28}, logistic regression analysis^{29,30,31}, random forest method^{32,33}, principal component analysis method^{34,35,36}, cell automata method^{37,38,39,40,41}. Likewise, although many researchers have noted that measuring and understanding the past, present, and future influences of urban growth and climate change, which is a key area of research and policy interest of ecological land conservation. But overly complicated simulation process has presented many unclear results with ongoing disagreement.

How to characterize the risk of degradation of ecological land caused by urban growth

remains a fundamental problem of future sustainable development, which has resulted in a widening debate^{42,43}. Due to convoluted social and natural factors, the fitness between morphology of urban growth and population size or density exhibits differences among various types of cities. However, related to assessment approaches may exhibit defects in the combined with climate change and urban growth, because of these studies neglect the interactions among different factors in complex urban system. Hence, capturing the dynamic features of urban growth is formulated to open a new avenue for strategic analysis of ecological land conservation in terms of the interplay among urban elements and it has a broad range of applications. The latest research has identified urban growth to climate change sensitive can determined by urban structure, with a new simulation method using population change as surrogate to urban structure. Besides alone physics indicators, this method resolves how to capture scale change phenomena associated with urban dynamics⁴⁴.

The ecological land' states significantly associate with urban growth and climate change over space and time. Ecological land conservation has long been recognized effective nature-based mitigation climate change and anthropogenic adaptation climate change of urban strategies, but estimation related to costs and benefits of urban interest groups facing uncertain risk scenarios remain little understanding⁴⁵. To this end, we start by revisiting how population scaling with size and density approaches have been investigated urban CO₂ emissions and urban heat island effect. Then, we devise a virtual city model to widely explain urban conservation strategies for ecological land in the real world. Although we only simulate as an example of Beijing, our method is a general form and can also be used to analyze other cities, especially mega-cities areas in developing or poor countries, where population is over agglomerated. Our model shows a combined speed of urban form change and climate change by linking demographic dynamic gravity, UHI intensity. We further build on this context to derive a series of conservation strategies on the ecological land under different risk scenarios, combining with multiple dimensions of urban growth and climate change.

Results

Climate change associated with urban scaling. The rapid increase of urban population is the main factor of urban growth. There is a strong power-law relationship between population size or density and climate change^{46,47}. Similarly, we used these approaches to investigate CO₂ emissions and urban heat island effect (see “Methods” section). Our work is motivated by a desire to use links between urban scaling hypotheses and climate change to identify relevant indicators of urban morphological change, and further modeling for economic analysis of ecological land conservation strategies.

Because of the universal significance of our model, we selected a typical mega-city with a large population in developing country as a case study. Fig.1 exhibits the scatter plot of the observed values of CO₂ emissions over 1986-2016 in Beijing. Our estimations describe that CO₂ emissions and population size show positive correlation (Fig.1a), CO₂ emissions and population density show negative correlation (Fig.1b). α_1 and β_1 indicate a sublinear law between CO₂ emissions and population size or density, so they mean that 1% increase in population size of Beijing associates with 0.79% in its CO₂ emissions, and 1% increase in population density of Beijing associates with -0.28% in its CO₂ emissions. Furthermore, population size change has greater effect on CO₂ emissions than population density.

If decreasing population density is benefit to mitigation of CO₂ emissions, this proves population size must be correlation to built-up area. From this point of view, developing compact cities with lower density and protecting ecological land is clearly conducive to the improvement of the overall urban heat environment^{48,49}. In contrast, single considering population size will lead to worse urban thermal environment^{50,51}.

a

b

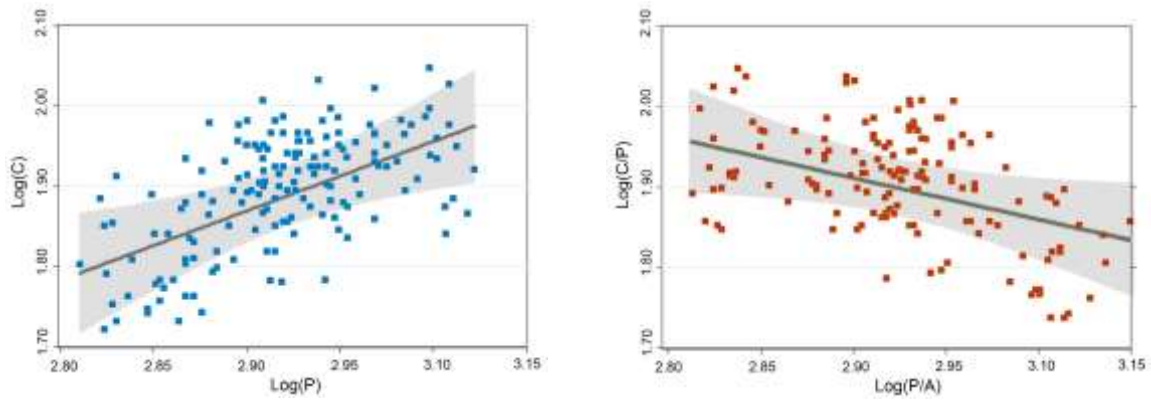


Fig.1 Investigating CO₂ emissions associated with urban scaling. **a** population size scaling on urban CO₂ emissions.

p -value = 0, $\bar{\alpha}_1 = 0.79 \pm 0.01$. Dark gray regression line and light gray envelope show 95% confidence interval. **b** population density

scaling on urban CO₂ emissions. p -value = 0, $\bar{\beta}_1 = -0.28 \pm 0.01$. Dark gray regression line and light gray envelope show 95%

confidence interval

The climate stress mainly indicates urban heat island effect, this effect is generally thought to be biophysical in nature, expressed by from large different temperature between rural and downtown. This heat effect is mainly measured by population density^{52,53}. Because of the small difference of long-term temperature observations in the same city, we use the cross-sectional temperature observation data of several cities in Beijing-Tianjin-Hebei region. From Fig.2, the variance of estimation results in winter is greater than variance of summer results. Importantly, the result show that the higher population density, the stronger urban heat island effect, which contradicts the measurement of CO₂ emissions. Therefore, we believe that the interaction effect between urban population and land needs to be studied by introducing relative measurements of comprehensive change.

a Sample cities

b Summer UHI / Winter UHI

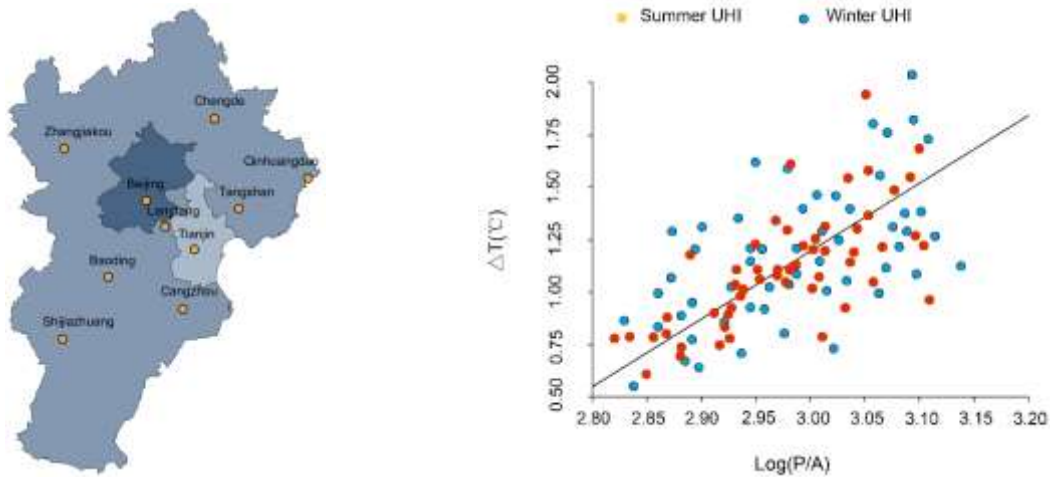


Fig.2 The relationship between population density and UHI. **a** Beijing-Tianjin-Hebei region is one of the regions with the densest distribution of population in China, and it is also significantly affected by climate change. The rapid process of urbanization has led to thermal environmental problems such as the heat island effect in this region. Central and nodal cities are shown in yellow dots. **b** Per capita density scaling: the scaling law between temperature difference and population density. There is extensive empirical evidence that urban growth associated with population agglomeration and urban built-up area expansion is the main factor affecting the heat island effect. Due to the influence of seasonal differences, we chose two seasons with obvious contrast between summer and winter to measure the urban heat island effect (see “Methods” section).

Allometric urban modelling. Accurately capturing the dynamic characteristics of urban growth plays central role in the establishment of ecological land conservation analysis. Therefore, we devise an upgraded gravitational cell model of urban growth (see “Methods” section). Our model is different from previous study in that it is a city simulation with growth constraints⁵⁴. Importantly, our idea is that sites close to the original core (such as downtown) are more likely to be occupied, while distant sites (such as suburb) remain largely empty. This description can explicitly show that the typical population distribution of most mega-cities in East Asia, Southeast Asia, and Africa.

In our module of urban growth, we explore an iteratively incrementing urban cell counts under different risk scenarios. Introducing risk scenarios describe possible future socio-economic, demographic, and environmental conditions is a commonly used method. The simulation based on scenarios limited by urban growth could promotes the applications in ecological land pattern changes studies. However, the precise shape of the risk curve is unclear

for complicated urban system. To make the comparison clearly, we only introduce low-risk and high-risk scenarios to simulation for monocentric urban cell growth. The low-risk scenario represents relative slower speed of urban growth, low population growth, and preference for environmentally friendly lifestyles reduce the demand for developing ecological land. In this case, a big city could improve green technologies can provide a compact and relative efficient urban spatial planning. In contrast, the high-risk scenario represents higher speed of urban growth with inequality and competition across countries or regional, these mega-cities expand to increase the demand for developing ecological land. In this case, the relationship between land use and population growth decreases fitness for environment. Fig. 3 describes the risk threshold value distribution under two scenarios.

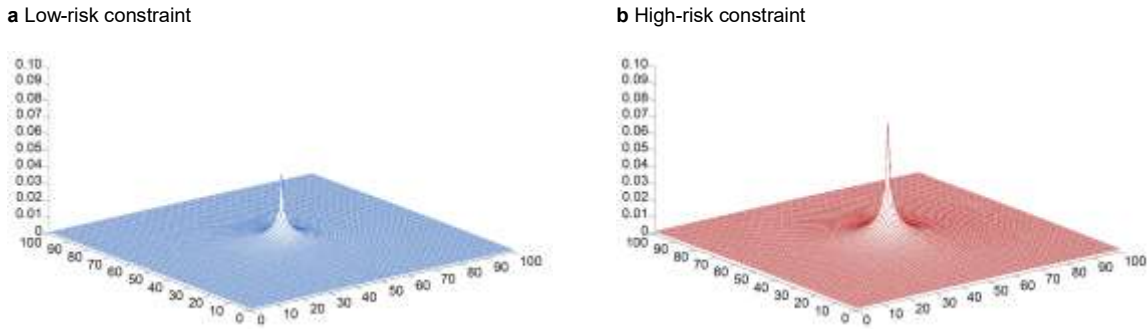


Fig.3 Threshold distribution. Based on relevant literatures and annual statistical yearbooks, we show an approach to simulate constraint conditions of urban growth under two risk pathways. **a** Low-risk scenario simulates relative sustainable urban development. the higher technical transformation enhances the climate adaptability of cities at all levels in the region, and the synergistic effect reduces the risk loss caused by urban excessive growth, which is conducive to the formation of a more compact city. Because the balanced development of cities in region, the disordered city structure caused by population migration and expansion of built-up areas is limited. **b** High-risk scenario simulates a more competitive environment among cities in the region. The population migration is unbalanced and gravitational effect of big cities is significant. Urban population are vulnerable to climate change and are less adaptable. The mismatch of resources among cities in the region results in a large amount of carbon emissions. With exacerbating land-use, cities are easy to form a loose and inefficient spatial layout. If $z < p_c$, then $v_{i,j}$ is cyclically accumulating in each iteration ($v_{i,j} \rightarrow v_{i,j} + m$), where z is a random variable matrix (100×100) between 0 and 1. $p_c (0 < p_c \leq 1)$ represents threshold value of cell growth affected by urban expansion under different risk scenarios, we set the occupation probability distribution function is

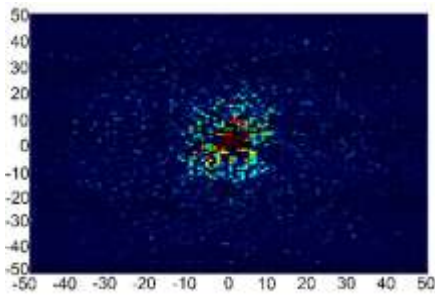
$$p_c = \frac{\alpha \times (1 - M)}{1 + e^{\alpha \times d}}$$

, where M represents the adjusted proportion parameter of future ecological land around a big city, α represents

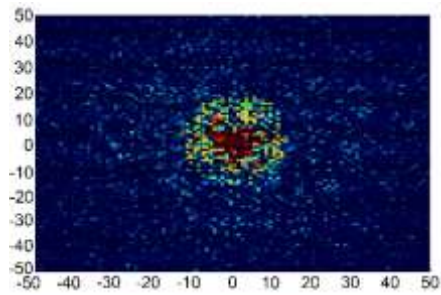
population growth speed comprehensive parameter under different scenarios. Reference to relevant literatures, we set a series of parameters $M_{low-risk} = 0.411$, $\alpha_{low-risk} = 0.04$ and $M_{high-risk} = 0.279$, $\alpha_{high-risk} = 0.06$ ^{55,56}.

Fig.4 shows that the evolutionary difference of urban cell counting and cluster expansion by tuning overall growth and radial decaying in the model under controlled two risk-threshold value scenarios. Our results show that the monocentric cluster in low-risk scenario is more compact than high-risk scenario, its scale evolves smaller, and the proliferating accumulation of urban cell per square kilometers is lower.

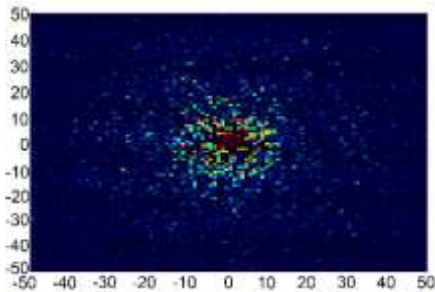
a $g = 0.2, \delta = 2.5$



c $g = 0.2, \delta = 2.5$



b $g = 0.7, \delta = 1.5$



d $g = 0.7, \delta = 1.5$

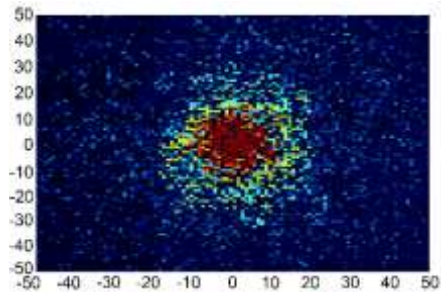


Fig.4 Examples of urban cell growth simulation. **a** and **b** show that urban growth in low-risk scenario. **c** and **d** show that urban growth in high-risk scenario. We put 2000 cumulative proliferating urban cells into the system square grid for 10 iterations and consider population counts in each grid, the procedure is repeated and stopped before the monocentric cluster reaches any boundaries of urban system.

We generate some modeling details. Fig.5a and Fig.5b show that a three-dimensional illustration of cell growth in hypothetical urban system resembling real world.

a

b

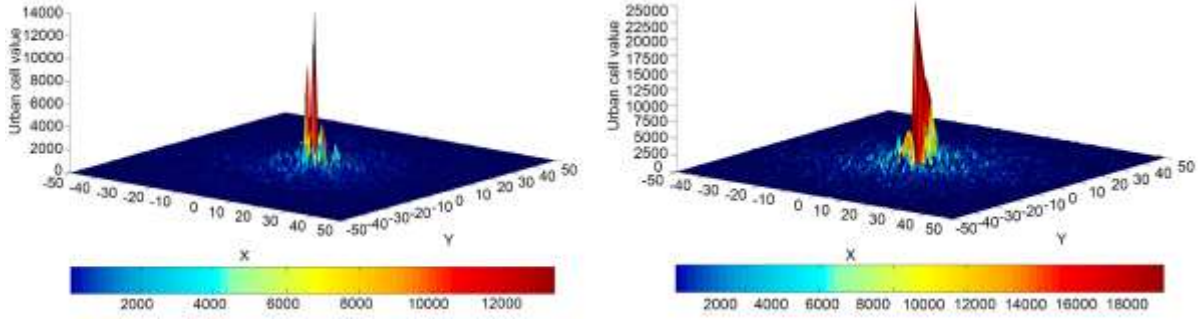


Fig.5 Three-dimensional urban cell growth for simulating mono-centric city. **a** urban growth in low-risk scenario. **b** urban growth in high-risk scenario. For each risk scenario, we repeated the simulation 30 times using the relevant default dataset.

Modeling urban dynamics and risk. Initially, we describe urban growth dynamics by a game.

The game is played by N ecological land grids over Ω rounds respective at one-dimensional linear space $X = 1, L, N$. In each round, the only ecological land grid near the urban boundary is under the threat of direct occupation. In each round $R = 1, 2, L$, we assume that urban must pay for a cost $c_{N,i}$ for conserving an ecological land grid i , where N represents the total number ecological land grids along remaining in the current round game in space system, and i represents each ecological land grid of distance to the urban boundary (Fig.6a). Then, a collective pot $\sum_{i=1}^N c_{N,i}$ represents the urban total cost to maintain overall ecological land grids.

Here, we propose urban expansion with linear law, except for the ecological land grid adjacent to the urban boundary all other ecological land grids are safe in each round game (Fig.6b). One hand, if urban growth control is successful, we set that each ecological land grid also will get a generalized benefit $b_{N,i}$. On the other hand, if the urban growth control is unsuccessful, urban will invade the frontier ecological land grid, any other ecological land grid is not on the frontier can gets benefit in this round, but importantly its distance to urban boundary will decrease by one in the next round.

To shed further light on collective conservation actions given such uncertainty, we use a joint method to measure the risk, which combines climate change, growth spatial gradient, and radial decay^{57,58,59}. The Eq.1 is inspired by related reference⁶⁰, this approach translates single estimates of temporal growth rates into joint estimates of combined speeds on urban spatial

morphology and urban climatic changing.

$$\frac{\text{Spatial gradient}}{\text{Temporal anomalies}} = \frac{\delta}{\Delta^{\circ}\text{C} \times g} \quad (1)$$

where $\Delta^{\circ}\text{C}$ represents annual and seasonal means of daily and nighttime averages temperature differences between downtown to suburb (see “Methods” section). We set the probability function on urban growth risk control is shown in Eq.2 and Fig.6c, this function $f(c)$ is assumed an increasing function with cost increase, where c represents conservation cost (see “Methods” section).

$$f(c) = \frac{\frac{\delta}{\Delta^{\circ}\text{C} \times g} \times c}{1 + \frac{\delta}{\Delta^{\circ}\text{C} \times g} \times c}, \text{ and } \frac{\delta}{g} > 0 \quad (2)$$

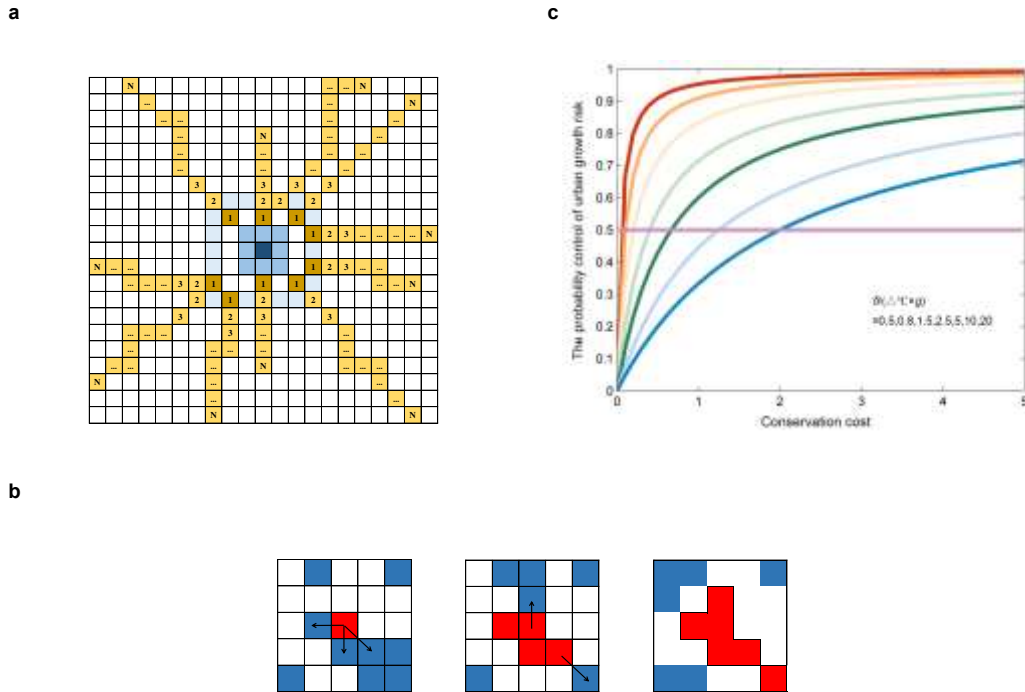


Fig.6 urban dynamics and risk. **a** Linear dynamics of urban space. **b** the Vulcan law on encroachment. **c** risk function.

Discount choice. The cost-benefit analysis of limited resources in future uncertain risks always involves the ethical choice problem of intergenerational equity. Therefore, we bring the time factor into the analysis process of ecological land conservation by introducing discount. Considering the similar influence of environmental Ramsey’s law, we set the discount factor η ,

where $0 \leq \eta \leq 1$. It represents the benefit of each ecological land grid in round r is weighted by η^{r-1} , simplicity let the discount factor is the same for all ecological land grids. When $\eta = 0$, it means that urban decision maker only cares about the current round game. When $\eta = 1$, it means that urban decision maker will equally care about all round games. Then, we get an infinite series $\sum_{r=1}^{\infty} \eta^{r-1} = \frac{1}{1-\eta}$. For example, if $\eta = 0.6$, then urban decision maker will care about 12.5 years in the future (Reference to the cycle of government decision-making on urban development in China, we assume 5 years urban planning per round game).

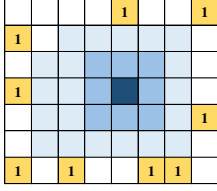
Cost strategies on ecological land conservation. Let each ecological land grid' benefit minus cost and maximize its profit. Besides, we will be faced with two situations of urban growth risk in each round game: one situation, urban growth control is successful in round $r = 1$, then each ecological land grid will face the same game situation in the next round. We propose a key property that the conservation strategies on each ecological land generally depends on distance to urban boundary and total number of ecological land grids remaining in the game. Another situation, we assume that urban growth control failed, then urban will invade frontier ecological land grid in current round, the total number of ecological land grids of remaining decrease to $N-1$, specially the distance to urban boundary of ecological land grid i is $i-1$. For the city, the situation faced by either ecological land grid i or ecological land grid $i-1$ in the next round game is the same, except that the initial location of urban boundary is different. The cost strategy of ecological land grid i is an i -dimension strategy profile, in total N ecological land grids game $c_{N,i} = (c_{N,i}, c_{N-1,i-1}, L, c_{N-i+1,1})$, where $1 \leq i \leq N$. We have a set of cost strategies for ecological land grid conservation, which is a Nash equilibrium strategy, as shown in Eq.3.

$$b_{N,i}^*(c_{N,1}^*, L, c_{N,i-1}^*, L, L, c_{N,i}^*, L, c_{N,i+1}^*, L, c_{N,N}^*) \geq S'_{N,i}(c_{N,1}^*, L, c_{N,i-1}^*, L, L, c'_{N,i}, L, c_{N,i+1}^*, L, c_{N,N}^*) \quad (3)$$

Naturally, for a certain ecological land grid, the city will not deviate from this Nash equilibrium cost strategy profile, because given that the cost strategy of other ecological land grids is unchanged, any other cost strategy will not be the optimal response for this ecological

grid.

Small-scale ecological land grids' strategies at urban boundary.



We firstly discuss only one ecological land grid, which is adjacent to urban boundary. The city will pay for a cost for ecological land grid $c_{1,1}$, related strategy is $s_{1,1}$. If we can successfully control urban growth in the first round, urban will face

the same situation the next round. We will have a benefit from the ecological land grid, as shown in from Eq.4 to Eq.6.

$$b = \left(\frac{\frac{\delta}{\Delta^\circ C \times g} \times c}{1 + \frac{\delta}{\Delta^\circ C \times g} \times c} \right) \times (1 + \eta \times b) - c \quad (4)$$

where $\eta \times b$ represents the benefit of ecological land grid in the second round. Solving for

b , we maximize this equation.

$$b = \frac{\left(\frac{\frac{\delta}{\Delta^\circ C \times g} \times c}{1 + \frac{\delta}{\Delta^\circ C \times g} \times c} \right) - c}{1 - \eta \times \left(\frac{\frac{\delta}{\Delta^\circ C \times g} \times c}{1 + \frac{\delta}{\Delta^\circ C \times g} \times c} \right)} \quad (5)$$

Differentiating with respect to c , we have:

$$b' = \frac{\eta \times \left(\frac{\frac{\delta}{\Delta^\circ C \times g} \times c}{1 + \frac{\delta}{\Delta^\circ C \times g} \times c} \right) + \left(\frac{\frac{\delta}{\Delta^\circ C \times g} \times c}{1 + \frac{\delta}{\Delta^\circ C \times g} \times c} \right)' - \eta \times \left(\frac{\frac{\delta}{\Delta^\circ C \times g} \times c}{1 + \frac{\delta}{\Delta^\circ C \times g} \times c} \right)' - 1}{\left(1 - \eta \times \left(\frac{\frac{\delta}{\Delta^\circ C \times g} \times c}{1 + \frac{\delta}{\Delta^\circ C \times g} \times c} \right) \right)^2} \quad (6)$$

Considering $P(c)$ as in Eq.4, we can calculate that for $\eta < 1$, we have Eq.7 and Eq.8.

$$c^* = \begin{cases} \frac{\sqrt{\eta + \frac{\delta}{\Delta^\circ C \times g} - \frac{\delta}{\Delta^\circ C \times g} \times \eta} - 1}{(1-\eta) \times \frac{\delta}{\Delta^\circ C \times g}} & \text{if } \frac{\delta}{\Delta^\circ C \times g} > 1 \\ 0 & \text{if } \frac{\delta}{\Delta^\circ C \times g} \leq 1 \end{cases} \quad (7)$$

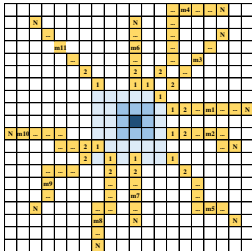
$$b^* = \begin{cases} \frac{1 + \eta + \frac{\delta}{\Delta^\circ C \times g} - \eta \times \frac{\delta}{\Delta^\circ C \times g} - 2 \times \sqrt{\eta + \frac{\delta}{\Delta^\circ C \times g} - \eta \times \frac{\delta}{\Delta^\circ C \times g}}}{(1-\eta)^2 \times \frac{\delta}{\Delta^\circ C \times g}} & \text{if } \frac{\delta}{\Delta^\circ C \times g} > 1 \\ 0 & \text{if } \frac{\delta}{\Delta^\circ C \times g} \leq 1 \end{cases} \quad (8)$$

When $\eta=1$, we have:

$$\left\{ \begin{array}{l} b^* = \frac{(\frac{\delta}{\Delta^\circ C \times g} - 1)^2}{4 \times \frac{\delta}{\Delta^\circ C \times g}} \\ c^* = \frac{\frac{\delta}{\Delta^\circ C \times g} - 1}{2 \times \frac{\delta}{\Delta^\circ C \times g}} \end{array} \right. \quad (9)$$

We find that when $\frac{\delta}{\Delta^\circ C \times g} > 1$, the city will pay for the ecological land grid with the optimum strategy c^* , as Eq.7, increasing with intergenerational discount η . It means that the city has farsighted for sustainability development concept on land use. Eq.9 represents urban growth successfully control case $f(c) = \frac{\frac{\delta}{\Delta^\circ C \times g} - 1}{1 + \frac{\delta}{\Delta^\circ C \times g}}$ (Simulation case see ‘‘Methods’’ section).

Large-scale ecological land grids’ strategies at urban boundary.



We can recursively establish the Nash equilibrium of N - ecological land grids in game. For ecological land grid i , its benefit is $b_{N,i}$, its cost is $c_{N,i}$. All ecological land grids at the Nash equilibrium strategy in an m ecological land grids game ($1 \leq m \leq N-1$) once the number of remaining ecological land grids

are m . Herein, we consider $\{c_{N,i}\}_{i=1, \dots, N}$ iid. To calculate the Nash equilibrium cost strategy of

ecological land grid i , we set the city will adopt the best response to other ecological land grids. If the Nash equilibrium cost strategies $\{c_{N,j}^*\}_{j \neq i}$, we consider ecological land grid at urban boundary, which will be paid by the city cost $c_{N,1}$. If urban growth control is successful in the current round game, then ecological land grid at urban boundary will faces the same situation in the next round game. Otherwise, the ecological land grid can be occupied by city.

$$b_{N,1}(c_{N,1}, c_{N,2}^*, \mathbf{L}, c_{N,N}^*) = \left[\frac{\frac{\delta}{\Delta^\circ C \times g} \times (c_{N,1} + \sum_{j \neq 1} c_{N,j}^*)}{1 + \frac{\delta}{\Delta^\circ C \times g} \times (c_{N,1} + \sum_{j \neq 1} c_{N,j}^*)} \right] \times (1 + \eta \times b_{N,1}) - c_{N,1} \quad (10)$$

From Eq.10, we have:

$$b_{N,1} = \frac{\left[\frac{\frac{\delta}{\Delta^\circ C \times g} \times (c_{N,1} + \sum_{j \neq 1} c_{N,j}^*)}{1 + \frac{\delta}{\Delta^\circ C \times g} \times (c_{N,1} + \sum_{j \neq 1} c_{N,j}^*)} \right] - c_{N,1}}{1 - \eta \times \left[\frac{\frac{\delta}{\Delta^\circ C \times g} \times (c_{N,1} + \sum_{j \neq 1} c_{N,j}^*)}{1 + \frac{\delta}{\Delta^\circ C \times g} \times (c_{N,1} + \sum_{j \neq 1} c_{N,j}^*)} \right]} \quad (11)$$

Considering ecological land grid $i, i > 1$ (Non-adjacent urban boundary), if the urban growth control is successful in the current round game, then the ecological land grid i will faces the same situation in the next round game with the distance to urban boundary $i-1$ and all ecological land grids $N-1$. Similarly, we have:

$$b_{N,i}(c_{N,1}, \mathbf{L}, c_{N,i}^*, \mathbf{L}, c_{N,N}^*) = \left[\frac{\frac{\delta}{\Delta^\circ C \times g} \times (c_{N,i} + \sum_{j \neq 1} c_{N,j}^*)}{1 + \frac{\delta}{\Delta^\circ C \times g} \times (c_{N,i} + \sum_{j \neq 1} c_{N,j}^*)} \right] \times (1 + \eta \times b_{N,i}) + (1 + \eta \times b_{N-1,i-1}^*) \times \left[1 - \left(\frac{\frac{\delta}{\Delta^\circ C \times g} \times (c_{N,i} + \sum_{j \neq 1} c_{N,j}^*)}{1 + \frac{\delta}{\Delta^\circ C \times g} \times (c_{N,i} + \sum_{j \neq 1} c_{N,j}^*)} \right) \right] - c_{N,i} \quad (12)$$

$$b_{N,i} = \frac{1 + \left[1 - \frac{\frac{\delta}{\Delta^\circ C \times g} \times (c_{N,i} + \sum_{j \neq 1} c_{N,j}^*)}{1 + \frac{\delta}{\Delta^\circ C \times g} \times (c_{N,i} + \sum_{j \neq 1} c_{N,j}^*)} \right] \times \eta \times b_{N-1,i-1}^* - c_{N,i}}{1 - \eta \times \left[\frac{\frac{\delta}{\Delta^\circ C \times g} \times (c_{N,i} + \sum_{j \neq 1} c_{N,j}^*)}{1 + \frac{\delta}{\Delta^\circ C \times g} \times (c_{N,i} + \sum_{j \neq 1} c_{N,j}^*)} \right]} \quad (13)$$

To find an internal solution for differentiating Eq.11 with respect to $c_{N,1}$, then we set $c^*_{N,i} > 0$ iid. We have the solution as show in Eq.14. Similarly, differentiating Eq.13 with respect to $c_{N,i}$, we have the solution as shown in Eq.15.

$$\begin{aligned} & \left[1 - \eta \times \left(\frac{\frac{\delta}{\Delta^\circ C \times g} \times (c_{N,1} + \sum_{j \neq 1} c^*_{N,j})}{1 + \frac{\delta}{\Delta^\circ C \times g} \times (c_{N,1} + \sum_{j \neq 1} c^*_{N,j})} \right) \right]^2 \frac{\partial b_{N,1}}{\partial c_{N,1}} \\ &= -1 + \eta \times \left(\frac{\frac{\delta}{\Delta^\circ C \times g} \times (c_{N,1} + \sum_{j \neq 1} c^*_{N,j})}{1 + \frac{\delta}{\Delta^\circ C \times g} \times (c_{N,1} + \sum_{j \neq 1} c^*_{N,j})} \right) + \left(\frac{\frac{\delta}{\Delta^\circ C \times g} \times (c_{N,1} + \sum_{j \neq 1} c^*_{N,j})}{1 + \frac{\delta}{\Delta^\circ C \times g} \times (c_{N,1} + \sum_{j \neq 1} c^*_{N,j})} \right)' \end{aligned} \quad (14)$$

$$- \eta \times \left(\frac{\frac{\delta}{\Delta^\circ C \times g} \times (c_{N,1} + \sum_{j \neq 1} c^*_{N,j})}{1 + \frac{\delta}{\Delta^\circ C \times g} \times (c_{N,1} + \sum_{j \neq 1} c^*_{N,j})} \right)' \times c_{N,1}$$

$$\left[1 - \eta \times \left(\frac{\frac{\delta}{\Delta^\circ C \times g} \times (c_{N,i} + \sum_{j \neq 1} c^*_{N,j})}{1 + \frac{\delta}{\Delta^\circ C \times g} \times (c_{N,i} + \sum_{j \neq 1} c^*_{N,j})} \right) \right]^2 \frac{\partial b_{N,i}}{\partial c_{N,i}} \quad (15)$$

$$\begin{aligned} &= -1 + \eta \times \left(\frac{\frac{\delta}{\Delta^\circ C \times g} \times (c_{N,i} + \sum_{j \neq 1} c^*_{N,j})}{1 + \frac{\delta}{\Delta^\circ C \times g} \times (c_{N,i} + \sum_{j \neq 1} c^*_{N,j})} \right) + \eta \times \left(\frac{\frac{\delta}{\Delta^\circ C \times g} \times (c_{N,i} + \sum_{j \neq 1} c^*_{N,j})}{1 + \frac{\delta}{\Delta^\circ C \times g} \times (c_{N,i} + \sum_{j \neq 1} c^*_{N,j})} \right)' \\ &- \eta \times c_{N,i} \times \left(\frac{\frac{\delta}{\Delta^\circ C \times g} \times (c_{N,i} + \sum_{j \neq 1} c^*_{N,j})}{1 + \frac{\delta}{\Delta^\circ C \times g} \times (c_{N,i} + \sum_{j \neq 1} c^*_{N,j})} \right)' - \eta \times b^*_{N-1,i-1} \times \left(\frac{\frac{\delta}{\Delta^\circ C \times g} \times (c_{N,i} + \sum_{j \neq 1} c^*_{N,j})}{1 + \frac{\delta}{\Delta^\circ C \times g} \times (c_{N,i} + \sum_{j \neq 1} c^*_{N,j})} \right)' \\ &+ \eta^2 \times b^*_{N-1,i-1} \times \left(\frac{\frac{\delta}{\Delta^\circ C \times g} \times (c_{N,i} + \sum_{j \neq 1} c^*_{N,j})}{1 + \frac{\delta}{\Delta^\circ C \times g} \times (c_{N,i} + \sum_{j \neq 1} c^*_{N,j})} \right)' \end{aligned}$$

For ecological land grid i , if $c^*_{N,i} = 0$, we have $\frac{\partial b_{N,i}}{\partial c_{N,i}} < 0$. For ecological land grid i , if

$c^*_{N,i} > 0$, then $\frac{\partial b_{N,i}}{\partial c_{N,i}} = 0$, we let Eq.14 and Eq.15 to zero.

Discussions

Cities are rapidly expanding in size, wealth, and power to our lived earth. Modern cities will become independent and stronger to determine how to plan urban morphologic growth autonomously because of their wealth. We find that even in ancient times, the excessive urban growth demands had led to magnitude degradation of environment. Finally, urban met collapse of wise civilization, such as degradation of ecological land around many cities in 3rd millennium BCE Mesopotamia⁶¹. Compared with the rate of urban growth today, we can imagine the crisis we are facing. Rapid urban growth of future trend in Africa, East Asia, and Southeast Asia is not optimistic to ecological land conservation. Mostly in the city that has an acute housing shortage, and where exuberant demand for land results in higher price, which has dire promotion on urban sprawl, informal land market⁶². It is even worse when the converted land is vacant in an inefficient and non-productive way. However, the contribution of land for economic development is substantial, for 45%-75% of wealth in some countries⁶³. In the face of the temptation of huge economic interests and the potential crisis of urban environmental survival, people always fall into the urban development dilemma of how to make decisions.

These crises are almost overwhelming and will require built autonomous ecological cities beyond traditional industrial and business for our future⁶⁴. When we are no longer so poor, we find that the ecological land is also a powerful selective force, urban conservation strategies alter behaviors, physiologies, and morphologies of dwellers. Substantially, Howard, Jacobs' philosophy of urban green seems to be a bit mechanical today, in our view, city as part of a complex set of environmental and social system and should be re-examined by the government. We should seek commonalities among city ecosystems, an understanding of ecological land conservation strategy how to shape the fitness on urban morphology between nature and humanity. Our objective explores what is likely to occur in city on ecological land conservation. We integrate the two dynamic modules on urban growth and climate change into the unified economic strategies on ecological land conservation, and this enriches the methods used in previous research.

Compact city is beneficial to reducing conservation cost. If $\eta = 1$, from Eq.14 and Eq.15, we have costs for all ecological land grids, as shown in Eq.16.

$$c^*_{N,1} = c^*_{N,2}, L, c^*_{N,N} = \frac{\frac{\delta}{\Delta^\circ C \times g} - 1}{\frac{\delta}{\Delta^\circ C \times g} \times (1 + N)} \quad (16)$$

Then we set $\frac{\delta}{\Delta^\circ C \times g} > 1$, we have ecological land grid' benefit located at the urban boundary, as shown in Eq.17.

$$b^*_{N,1} = \frac{(\frac{\delta}{\Delta^\circ C \times g} \times N^2 - 1) \times (\frac{\delta}{\Delta^\circ C \times g} - 1)}{(\frac{\delta}{\Delta^\circ C \times g}) \times (1 + N)^2} \quad (17)$$

As shown in Fig.7, our result show that developing compact city may reduce conservation cost for ecological land⁶⁵. This urban morphology means that the value of δ is relatively large and the value of g is relatively small. In addition, when $\frac{\delta}{g} = \text{constant}$, if $\Delta^\circ C$ is smaller, although the density of a city is higher, the heat island effect is lower. Because of urban weaker climate stress, it means that the compact urban spatial structure is more reasonable, by the control of building height and efficient block layout should play good role in alleviating thermal effect. The sustainable and rational developing of urban construction land will form scale effect of local environment. Population distribution and natural resources are in harmony with each other, which are conducive to conservation cost savings^{66,67}.

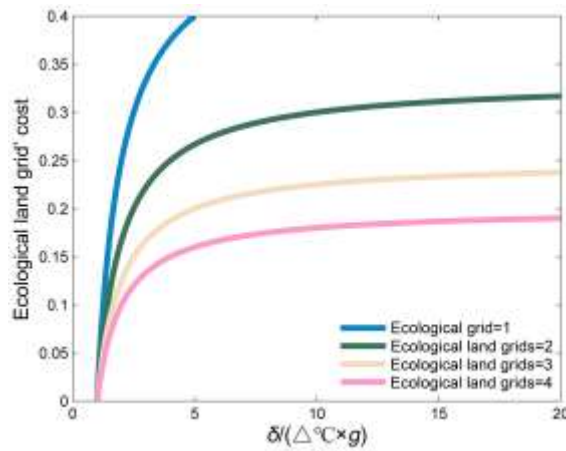


Fig.7 Difference of Cost caused by $\frac{\delta}{\Delta^\circ C \times g}$ ($\eta=1$).

Discount choice when the city is stable. When $\frac{\delta}{\Delta^{\circ}C \times g} > 1$ is constant, such as $\frac{\delta}{\Delta^{\circ}C \times g} = 2$, at this time, we think that the comprehensive state of urban growth and climate change is relatively stable for a big city. If the city chooses different intergenerational discount, as shown in Fig.8 and Eq.18, with the enlarging scale of conservation, the greater difference in cost payment. When the city only cares about the ecological land at the boundary, no matter how the discount is chosen, the difference of conservation cost is not obvious. Furthermore, we also find that if $\eta = 0, \frac{\delta}{\Delta^{\circ}C \times g} \leq 1$, then $c^*_{N,i} = 0$. This is an extreme situation, and city does not pay attention to ecological land conservation.

$$c^*_N = \frac{-1 + \sqrt{\frac{\delta}{\Delta^{\circ}C \times g} + \eta \times (1 + \frac{\delta}{\Delta^{\circ}C \times g} \times (-2 + \eta + N - \eta \times N - (1 - \eta)^2 \times b^*_{N-1}))}}{(\frac{\delta}{\Delta^{\circ}C \times g}) \times (1 - \eta)} \quad (18)$$

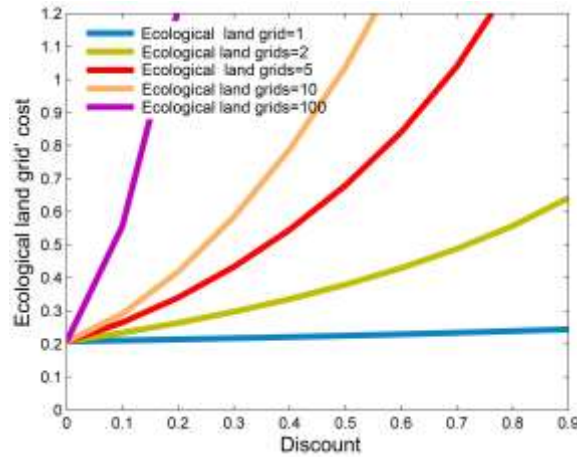


Fig.8 Ecological land grid' cost with different discount ($\frac{\delta}{\Delta^{\circ}C \times g} = 2$).

Optimizing of ecological land at urban boundary. We find that the city has strong adaptability to climate change, slow growth rate and large decay rate. At this situation, the urban spatial structure is more compact and reasonable, the erosion risk of ecological land at the urban boundary is lower, as shown in Fig.9 and Eq.19. But it has little relation between the erosion risk of ecological land at urban boundary and the overall conservation scale of ecological lands.

$$p(\sum_j c_{N,j}^*) = \frac{(\frac{\delta}{\Delta^\circ C \times g} - 1) \times \frac{N}{1+N}}{1 + (\frac{\delta}{\Delta^\circ C \times g} - 1) \times \frac{N}{1+N}} \quad (19)$$

Fig.10 shows that the benefit of ecological land grid at urban boundary. We simulation 0-100 grids, the benefit of ecological land grid at urban boundary tends to be stable with the increase of the total scale. Similarly, when combined speeds ($\frac{\delta}{\Delta^\circ C \times g}$) are larger, it also represents compact city as the above explanations, these factors will increase ecological land grid' benefit at urban boundary.

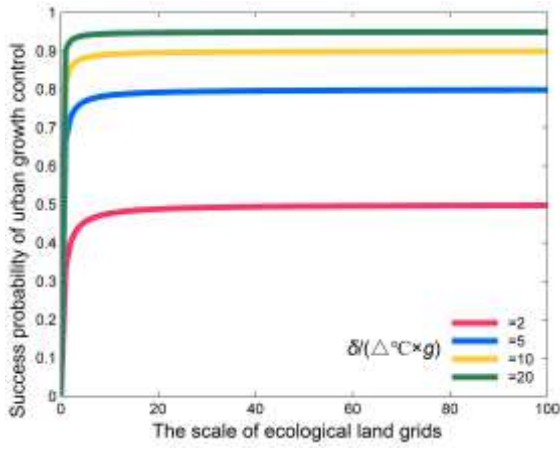


Fig.9 Urban growth risk.

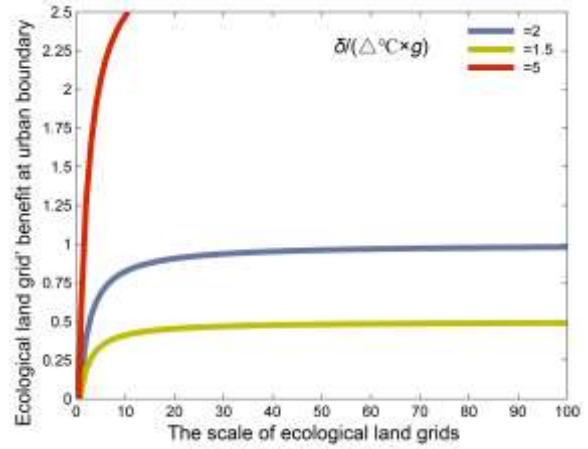


Fig.10 Ecological land grid' benefit at urban boundary.

Cost threshold effect of ecological land conservation. We propose a general solution of Nash equilibrium cost of ecological land grids, as shown in Eq.20 and Eq.21.

$$c_{N,1}^* = \frac{\sqrt{\frac{\delta}{\Delta^\circ C \times g} + \eta - \frac{\delta}{\Delta^\circ C \times g} \times \eta + \sum_{j \neq 1} c_{N,j}^* \times \frac{\delta}{\Delta^\circ C \times g} \times \eta \times (1-\eta) - 1}}{\frac{\delta}{\Delta^\circ C \times g} \times (1-\eta)} - \sum_{j \neq 1} c_{N,j}^* \quad (20)$$

$$c_{N,i}^* = \frac{\sqrt{\eta - \frac{\delta}{\Delta^\circ C \times g} \times \eta - \frac{\delta}{\Delta^\circ C \times g} \times \eta^2 - b_{N-1,i-1}^* \times \frac{\delta}{\Delta^\circ C \times g} \times \eta \times (1-\eta)^2 + \sum_{j \neq i} c_{N,j}^* \times \frac{\delta}{\Delta^\circ C \times g} \times \eta \times (1-\eta)}}{\frac{\delta}{\Delta^\circ C \times g} \times (1-\eta)} - \sum_{j \neq i} c_{N,j}^* \quad (21)$$

For general solution case, as shown in Fig.11 and Fig 12, our results indicate that a big city has two discount threshold effect of cost η_{orange}^* and η_{green}^* . For interaction between two piece of ecological land grids in a game, if $\eta < \eta_{orange}^*$, the city will not pay for ecological land grid 2, only ecological land grid 1 of cost will be paid. If $\eta \geq \eta_{orange}^*$, then the city begins to pay

for ecological land grid 2 of cost. When $\frac{\delta}{\Delta^{\circ}C \times g} = 2$, then $\eta^*_{orange} = 0.74$. When $\frac{\delta}{\Delta^{\circ}C \times g} = 15$, then $\eta^*_{orange} = 0.86$. Besides, if $\eta \geq \eta^*_{green}$, then the costs of two piece of ecological land grids will quickly converge to the unique Nash equilibrium solution when facing with long-term discount choice. Our results show that the less climate pressure, the more compact and rational layout of cities (the higher value of $\frac{\delta}{\Delta^{\circ}C \times g}$) will have more higher expectation of the welfare fairness of ecological land (the higher threshold effect). Importantly, when the city focuses on future ecological land resources, the conservation costs of boundaries do not increase. This result describes the sustainability of ecological land conservation is reduced.

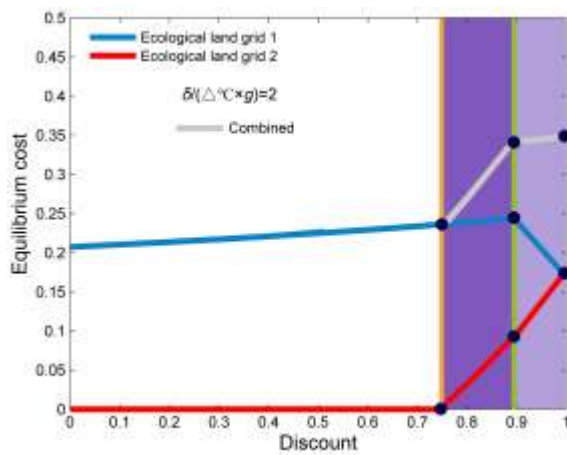


Fig.11 The Nash equilibrium cost

(two piece of ecological land grids).

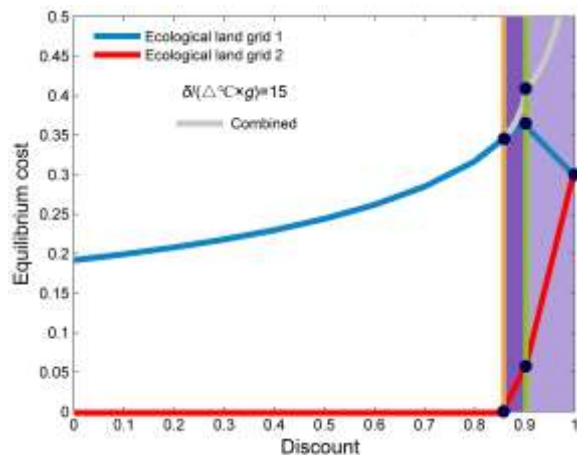


Fig.12 The Nash equilibrium cost

(two piece of ecological land grids).

Many unsettled questions about the negative impacts of urban growth and climate change. It is unclear how fast the global process of severe erosion of ecological land. Many unreasonable decisions of urban land-use do not have to a direct and temporal severe loss but only affect urban dwellers in the future.

Our study aimed at exploring strategic choices on ecological land conservation linking with complex interactions between urban growth and climate change. We confirm that reasonable limits of urban growth and enhancing adaption of climate change will reduce conservation cost and risk for ecological land. This study reveals that comprehensive impact on ecological land conservation from demographic distribution and temperature difference in

urban-rural system. City-level strategies of ecological land conservation aimed at reducing warming and optimizing urban spatial structure should account for these inherent nonlinear changes of city gravity.

Our analytical approach is general and could be used to assess in other cities. However, there are still several limitations in our work. We have not identified the heterogeneity among different ecological land grids and lack explicit scaling division of ecological land grid by combing statistical and remote data. Simultaneous, our modeling is relatively rough without considering other social-economic ingredients, and only introducing singly urban heat island effect on climate change. Despite of these limitations, our study adds to the current understanding about the role of a big city on ecological land conservation, shedding light particularly upon the space driving of urban growth and climate change. Finally, because of the fairness issues on future welfare, we show that discount decision plays still dominant core in urban contributions of ecological land conservation when facing potential risks.

Methods

Population size and density scaling of CO₂ emissions. Here, population size (P) and built-up area (A) as two key independent variables introduced, we have applied the usual least-squares method to the relationship between urban aggregated CO₂ emissions and population size and density scaling, as shown in Eq.22 and Eq.23. Similarly, we also have applied the same method to measure the relationship between temperature difference and population density, as shown in Eq.24.

$$\text{Log}C = \text{cons} + \alpha_1 \times \text{Log}P \quad (22)$$

$$\text{Log} \frac{C}{P} = \text{cons} + \beta_1 \times \text{Log} \frac{P}{A} \quad (23)$$

$$\Delta T = \text{cons} + \gamma_1 \times \text{Log} \frac{P}{A} \quad (24)$$

where, α_1 , β_1 , γ_1 are independent parameters, C represents urban CO₂ emissions, ΔT represents temperature difference between downtown and rural.

Urban growth model. The model generates the process to future demographic change monocentric city under different risk scenarios. Monocentric city modelling still plays a key role in urban development

research at present stage. Here, the concept of virtual urban is that we allow other small cluster to be generated within a certain area around the single core city located at the central point, which describes regional uncertainty of demographic migration in real world, such as the attraction effect on satellite town population flows. Starting with square grids of urban system size $N \times N$, where subscript (i, j) is site coordinate. A monocentric urban cell growth model is $V_{i,j} = \frac{g}{C_{i,j}} \times \sum v_{i,j}(m) \times d_{i,j}^{-\delta}$, we initially set a single cell $v_{0,0} = 1$ is occupied in the center of square grid and others are empty ($v_{i,j} = 0$). Where g ($0 < g \leq 1$) is the overall speed of cell growth, $C_{i,j} = 1$ is a special constant, reference⁶⁸. m represents cumulative reproduction times of cells, $d_{i,j}$ is the Euclidean distance between the grid (i, j) to center. δ is a key free exponent parameter, which determines that the urban gravity decaying with radical distance to the power law, range from 1.5 to 3, and close to Zipf's exponent. We set a series of parameter values, such as $g = 0.01, 0.02, 0.05, 0.1, 0.15, 0.2, 0.25, 0.5$ to better fit the simulation of a wide range of different population distribution patterns⁶⁹.

Combined speeds. For $\frac{\delta}{\Delta^\circ C \times g}$, when the intensity of the urban heat island effect increases, we have $0 < \frac{1}{\Delta^\circ C} < 1$. For example, Tab.1⁷⁰ shows annual and seasonal means of daily and nighttime averages of UHI intensity at Gongti CBD station to Daxing suburb station during 2009-2014 in Beijing.

Tab.1 Beijing Gongti CBD station of UHI (tensity/°C)						
Year	2009	2010	2011	2012	2013	2014
Annual mean	0.94(1.47)	0.92(1.55)	0.96(1.60)	1.01(1.65)	1.09(1.76)	1.20(1.91)
Summer mean	0.91(1.35)	0.88(1.31)	0.53(0.83)	0.73(1.21)	0.68(0.76)	1.16(1.79)
Autumn mean	1.14(1.90)	1.02(2.00)	1.23(2.21)	1.25(2.30)	1.19(2.20)	1.25(2.18)
Winter mean	1.12(1.90)	1.09(1.96)	1.18(2.09)	1.30(1.98)	1.53(2.58)	1.40(2.21)
Spring mean	0.49(0.74)	0.55(0.96)	0.73(1.28)	0.80(1.13)	0.97(1.52)	0.99(1.46)

The temperature difference values in parentheses represents the nighttime

The probability of urban growth risk. For $f(c) = \frac{\frac{\delta}{\Delta^\circ C \times g} \times c}{1 + \frac{\delta}{\Delta^\circ C \times g} \times c}$, when $f(0) = 0$, then it means that urban

does not pay for any ecological land grid and faces ongoing loss of ecological land. When $\lim_{c \rightarrow \infty} f(c) = 1$, it

represents the city has always controlled the current urban size and has been concerned with the conservation of all ecological land grids $f'(c) > 0$, and $f''(c) < 0$. First derivative of $f(c)$:

$$f'(c) = \frac{\frac{\delta}{\Delta^{\circ}C \times g}}{(1 + \frac{\delta}{\Delta^{\circ}C \times g} \times c)} - \frac{(\frac{\delta}{\Delta^{\circ}C \times g})^2 \times c}{(1 + \frac{\delta}{\Delta^{\circ}C \times g} \times c)^2}$$

Small-scale ecological land grids' strategies at urban boundary.

Simulation case:

If $\frac{\delta}{\Delta^{\circ}C \times g} = 7, \eta = 1$, so we have: every round, $b^* = \frac{9}{7}, c^*_{1,1} = \frac{3}{7}, f^*(c) = 0.75$, then it means that ecological land grid conservation will be sustainable for 15 years.

If $\frac{\delta}{\Delta^{\circ}C \times g} \leq 1$, then the ecological land grid does not be paid for anything, the threshold value is $\frac{\delta}{\Delta^{\circ}C \times g} = 1$. The marginal increase of the probability of urban growth control per unit cost around $c = 0$ is $f'(c) = \frac{\delta}{\Delta^{\circ}C \times g}$, the marginal increase of benefit from per unit cost is also $\frac{\delta}{\Delta^{\circ}C \times g}$, we set yearly benefit is 1. Therefore, it is worth paying positive cost provided that the initial marginal return per cost $\frac{\delta}{\Delta^{\circ}C \times g}$ is greater than 1.

If a varied $\frac{\delta}{\Delta^{\circ}C \times g}$ and a fixed η , c^* will be maximized at $\frac{\delta}{\Delta^{\circ}C \times g} = 2 + \frac{2}{\sqrt{1-\eta}}$. We find that a higher

$\frac{\delta}{\Delta^{\circ}C \times g}$ value sometimes led to lower cost of ecological land conservation, but this can be explained as that when city is wealthy, compact, and high organic will lead to this case.

Study case and Dataset. Beijing is located in the north of North China Plain, the east of Beijing is adjacent of Tianjin, and the rest is surrounded by Hebei (Urban central position: 116° 20' E, 39° 56' N), where the climate is a typical semi-humid and semi-arid monsoon climate in warm temperature zone. Beijing is hot and rainy in summer, cold and dry in winter, short in spring and autumn. Beijing is surround by mountains in the west, north, and northeast, and in the southeast by plains. The average elevation of Beijing is 43.5meters. Beijing has a total area of 16410.54 square kilometers. By 2019, the resident population was 21.536 million and the urbanization rate was 86.6%. Beijing is the capital of the people's republic of China, which is a typical representative of emerging cities in developing countries and is rated as a world first-tier city by the

world authority-GaWC. Modern Beijing was found in the Yongle period of the Ming Dynasty, which bears the history of more than 600 years of human civilization. Fig.13 shows that Beijing' evolution of modern urban growth and its impact on the growth of surrounding cities (as the cases of Tianjin, Tangshan). This study relies on quantitative data from NASA Database, Global Carbon Budget Database, China CO₂ Emission Accounts (CEADS: from Nature-Scientific Data), ATLAS of Urban Expansion Database, China Meteorological Data Network Database, China City Statistical Yearbook, China Statistical Yearbook on environment. In our calculations, some of the data directly referenced the related results published by authoritative journals.

Beijing (1800-2013)

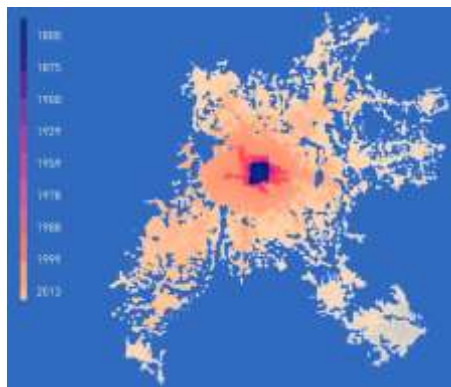


Fig.13 The evolutionary growth of Beijing (mono-centric form).

From: ATLAS of Urban Expansion Database

References

- ¹ Rosenzweig C., Solecki W., Hammer S.A., et al. Cities lead the way in climate-change action[J]. *Nature*,2010,467:909-911
- ² IPCC, 2014. Climate change 2014: Synthesis Report[R]. Cambridge University Press, Cambridge and New York,2014
- ³ Elmqvist, T., Anderson E., Frantzeskaki N., et al. Sustainability and resilience for transformation in the urban century[J]. *Nature Sustainability*,2019,2:267-273
- ⁴ UN. World urbanization process 2018[R]. New York: United Nations Department of Economic and Social Affairs (UN-DESA), Population Division,2018
- ⁵ Xinli Ke., Jasper Van Vliet., Ting Zhou., et al. Direct and indirect loss of natural habitat due to built-up area expansion: a mode-based analysis for the city of Wuhan China[J]. *Land Use*

Policy,2018,74:231-239

⁶ Junlong Huang, Zhuo Tang, Dianfeng Liu, et al. Ecological response to urban development in a changing socio-economic and climate context: policy implications for balancing regional development and habitat conservation[J]. *Land Use Policy*,2020,97:104772

⁷ Jones P.D., Lister D.H., Li Qingxiang. Urbanization effects in large-scale temperature records, with an emphasis on China[J]. *Geophysical. Research Letters*,2008,113(16):
<https://doi.org/10.1029/2008JD009916>

⁸ Linard C., Team A.J., Gilbert M. Modeling spatial patterns of urban growth in Africa[J]. *Applied Geography*,2013,44:23-32

⁹ Gang Xu, Ting Dong, Patrick B.C., et al. Urban expansion and form changes across African cities with a global outlook: Spatiotemporal analysis of urban land densities[J]. *Journal of Cleaner Production*,2019,224:802-810

¹⁰ Darmanto N.S., Varquez A.C., Kawano N., et al. Future urban climate projection in a tropical megacity based on global climate change and local urbanization scenarios[J]. *Urban Climate*,2019,29:100482

¹¹ Xiaoping Liu, Fengsong Pei, Youyue Wen, et al. Global urban expansion offsets climate-driven increase in terrestrial net primary productivity[J]. *Nature Communications*,2019,10:5558

¹² UN-Habitat. *Urbanization and Nations Human Settlements Programme*[R]. UN-Habitat, 2016.

¹³ Meehl G.A., Tebaldi C. More intense, more frequent, and longer lasting heat waves in the 21st century[J]. *Science*,2004,305:994-997

¹⁴ Mora C., Dousset B., Caldwell I.R., et al. Global risk of deadly heat[J]. *Nature Climate Change*,2017,7(7):501

¹⁵ Patz J.A., Campbell L.D., Holloway T., et al. Impact of regional climate change on human health[J]. *Nature*,2005,438:3101

¹⁶ Grimm N.B. Faeth S.H., Golubiewski N.E., et al. Global change and the ecology of cities[J] *Science*,2008,319:756-760

¹⁷ Rydin Y., Bleahu A., Davies M.E., et al. Shaping cities for health: complexity and the planning of urban environments in the 21st century[J]. *The Lancet*,2012,379:2079-2108

¹⁸ Grimmond S. Urbanization and global environmental change: Local effects of urban warming[J]. *Geographical Journal*,2007,173:83-88

- ¹⁹ Moore M., Gould P., Keary B.S. Global urbanization and impact on health[J]. *International Journal of Hygiene and Environmental Health*, 2003,206:269-278
- ²⁰ Yunzhi Zhang, Yunfeng Hu, Dafang Zhuang. A highly integrated, expansible, and comprehensive analytical framework for urban ecological land: A case study of Guangzhou, China[J]. *Journal of Cleaner Production*,2020,268:122360
- ²¹ Lambin E.F., Meyfroidt P. Global land use change, economic globalization, and the looming land scarcity[J]. *Proc.Natl.Acad.Sci.U.S.A.*,2011,108:3465-3472
- ²² Costanza R., Groot R.D., Sutton P., et al. Changes in the global value of ecosystem services[J]. *Global Environmental Change*,2014,26:152-158
- ²³ Martin Jung, Pedram Rowhani, Jörn P.W. Scharlemann. Impacts of past abrupt land change on local biodiversity globally[J]. *Nature Communications*,2019,10:5474
- ²⁴ Tubiello F.N., Salvatore M., Ferrara A.F., et al. The contribution of agriculture, forestry, and other land use activities to global warming[J]. *Global Change Biology*,2015,21:2655-2660
- ²⁵ Jasper van Vliet. Direct and indirect loss of natural area from urban expansion[J]. *Nature Sustainability*, 2019,2:755-763
- ²⁶ McPhearson T., Schinko T. Scientists must have a say in the future of cities[J]. *Nature*,2016,538(6310):290-292
- ²⁷ Scanches Fernandes L.F., Fernandes A.C.P., Ferreira A.R.L., et al. A partial least squares-path modeling analysis for the understanding of biodiversity loss in rural and urban watersheds in Portugal[J]. *Science of The Total Environment*,2018,626:1069-1085
- ²⁸ Vinicius S.R., Renato F.V., Luis F.S., et al. The assessment of water erosion using partial least square-path modeling: a study in a legally protected area with environmental land use conflicts[J]. *Science of The Total Environment*,2019,691:1225-1241
- ²⁹ Kumar R., Nandy S., Agarwal R., et al. Forest cover dynamics analysis and prediction modeling using logistic regression model[J]. *Ecological Indicators*,2014,45:444-455
- ³⁰ Modeling of urban growth in tsunami-prone city using logistic regression: analysis of Banda Aceh, Indonesia[J]. *Applied Geography*,2015,62:237-246
- ³¹ Macros R., Adrian J., Dhais P.A., et al. A comprehensive spatial-temporal analysis of driving factors of human-caused wildfires in Spain using geographically weighted logistic regression[J]. *Journal of Environmental Management*,2018,225:177-192
- ³² Shin Araki, Masayuki Shima, Kouhei Yamamoto. Spatiotemporal land use random forest

model for estimating metropolitan NO₂ exposure in Japan[J]. *Science of The Total Environment*,2018,634:1269-1277

³³ Sasanka G., Arijit D. Wetland conservation risk assessment of East Kolkata Wetland: a Ramsar site using random forest and support vector machine model[J]. *Journal of Cleaner Production*,2020,275:123475

³⁴ Hector A. Olvera, Mario Garcia, Wenwhai Li, et al. Principal component analysis optimization of a PM_{2.5} land use regression model with small monitoring network[J]. *Science of The Total Environment*,2012,425:27-34

³⁵ Yifan Wen, Hui Wang, Timothy Larson, et al. On-highway vehicle emission factors and spatial patterns based on mobile monitoring and absolute principal component score[J]. *Science of The Total Environment*,2019,676:242-251

³⁶ Ry Crocker, William H. Blake, Thomas H. Hutchinson, et al. Spatial distribution of sediment phosphorus in a Ramsar wetland[J]. *Science of The Total Environment*,2020,6:142749

³⁷ Lingqiang Kong, Guangjin Tian, Bingran Ma, et al. Embedding ecological sensitivity analysis and new satellite town construction in an agent-based model to simulate urban expansion in the Beijing metropolitan region, China[J]. *Ecological Indicators*,2017,82:233-249

³⁸ Mengyuan Jia, Yan Liu, Scott N. Lieske, et al. Public policy change and its impact on urban expansion: a evaluation of 265 cities in China[J]. *Land Use Policy*,2020,97:104754

³⁹ Xun Liang, Qingfeng Guan, Keith C. Clarke, et al. Mixed-cell cellular automata: a new approach for simulating the spatiotemporal dynamics of mixed land use structures[J]. *Landscape and Urban Planning*,2020,205:103960

⁴⁰ Charles P. Newland, Hedwigvan Delden, Aaron C.Zecchin, et al. A hybrid(semi)automatic calibration method for cellular automata land use models: combining evolutionary algorithms with process understanding[J]. *Environmental Modelling&Software*,2020,134:104830

⁴¹ Jianjun Lv, Yifan Wang, Xun Liang, et al. Simulating urban expansion by incorporating an integrated gravitational field model into a demand-driven random forest cellular automata model[J]. *Cities*,2021,109:103044

⁴² Bhatta B., Saraswati S., Bandyopadhyay D. Urban sprawl measurement from remote sensing data[J]. *Applied Geography*,2010,40(4):731-740

⁴³ Iraj Emadodin, Alireza Taravat, Masih Rajaei. Effects of urban sprawl on local climate: a

case study, north central Iran[J]. *Urban Climate*,2016,17:230-247

⁴⁴ Gabriele M., Simone F., Markus S., et al. Magnitude of heat islands largely explained by climate and population[J]. *Nature*,2019,573:55-60

⁴⁵ Austin K.G., Baker J.S., Sohngen B.L., et al. The economic costs of planting, preserving, and managing the world's forests to mitigate climate change[J]. *Nature Communications*,2020,11:5946

⁴⁶ Haroldo V., Ribeiro R., Jürgen P.K. Effects of changing population or density on urban carbon dioxide emissions[J]. *Nature communications*,2019,10,3204

⁴⁷ Gabriele Manoli, Simone Fatichi, Markus Schläpfer, et al. Magnitude of urban heat islands largely explained by climate and population[J]. *Nature*,2019,573:55-60

⁴⁸ Dodman D. Forces driving urban greenhouse gas emissions[J]. *Current Opinion in Environmental Sustainability*,2011,3:121-125

⁴⁹ Haozhi Pan, Jessica Page, Le Zhang, et al. Using comparative socio-ecological modeling to support Climate Action Planning (CAP) [J]. *Journal of Cleaner Production*,2019,232:30-42

⁵⁰ Stone B., Hess J.J., Frumkin H. Urban form and extreme heat events: are sprawling cities more vulnerable to climate change than compact cities?[J]. *Environmental Health Perspectives*,2010,118:1425-1428

⁵¹ Zhou B., Rybski D., Kropp J.P. The role of city size and urban form in the surface urban heat island[J]. *Scientific Reports*,2017,7:4791

⁵² Chang Cao, Xuhui Lee, Shoudong Liu, et al. Urban heat island in China enhanced by haze pollution[J]. *Nature Communications*,2016,7:12509

⁵³ Edwin Alejandro R.A., Lea Cristina L.S. Urban form and population density: influences on urban heat island intensities in Bogota, Colombia[J]. *Urban Climate*,2019,29:100497

⁵⁴ Yunfei Li, Schubert S., Kropp P.J., et al. On the influence of density and morphology on the Urban Heat Island intensity[J]. *Nature communication*,2020,11:2647

⁵⁵ Tong Jiang, Jing Zhao, Lige Cao, et al. Projection of national and provincial economy under the shared socioeconomic pathways in China[J]. *Climate change research*, 2018,14(1):50-58

⁵⁶ Guang Zhao Chen, Xia Li, Xiaoping Liu, et al. Global projections of future urban land expansion under shared socioeconomic pathways[J]. *Nature communications*,2020,11:537

⁵⁷ Loarie S.R., Duffy P.B., Hamilton H., et al. The velocity of climate change[J]. *Nature*,2009,462:1052-1055

- ⁵⁸ Ordonez A., Williams J. Projected climate reshuffling based on multivariate climate-availability, climate-analog, and climate-velocity analyses: implications for community disaggregation[J]. *Climatic Change*,2013,119:659-675
- ⁵⁹ Dobrowski S.Z., Abatzoglou J.T., Swanson A.K., et al. The climate velocity of the contiguous United States during the 20th century[J]. *Glob. Change Biol*,2013,19:241-251
- ⁶⁰ Ordonez A., Martinuzzi S., Radeloff V.C., et al. Combined speeds of climate and land-use change of the conterminous US until 2050[J]. *Nature Climate Change*,2014,4:811-816
- ⁶¹ Redman C.L. In human impact on ancient environments[M]. Tucson A Z, USA: The University of Arizona Press,1999:127-158
- ⁶² Lucy S. T., Donal B. Graham A. et al. Mapping changes in housing in sub-Saharan Africa from 2000 to 2015[J]. *Nature*,2019,568:391-406
- ⁶³ Nesru H. Koroso, Jaap A. Zevenbergen, & Monica Lengoiboni. Urban land use efficiency in Ethiopia: An assessment of urban land use sustainability in Addis Abba[J]. *Land Use Policy*,2020,99:105081
- ⁶⁴ Barbara Norman. Are autonomous cities our urban future?[J]. *Nature Communications*,2018,9:2111
- ⁶⁵ McGrath D. T. More evidence on the spatial scale of cities[J]. *Journal of Urban Economics*,2005,58(1):1-10
- ⁶⁶ Spivey C. The Mills-Muth model of urban spatial structure: Surviving the test of time?[J]. *Urban Studies*,2008,45(2):295-312
- ⁶⁷ Long Maoqian, Meng Xiaochen. Urbanization, suburbanization and China's urban spatial expansion[J]. *Areal Research and Development*,2015,34(3):54-60
- ⁶⁸ Rybski D., Ros AGC, Kropp P.J. Distance weighted city growth[J]. *Physical Review E*,2013,87(4):042114
- ⁶⁹ Yanjun Wang, Cheng Jing, Lige Cao, et al. The population patterns over China under the 1.5°C and 2.0°C warming targets[J]. *Climate change research*,2017,13(4):327-336
- ⁷⁰ Zhigang Cheng, Ju Li, Mingyu Zhou, et al. A study on urban heat island effect in Beijing central business district (CBD)[J]. *Climatic and Environmental Research*,2018,23(6):633-644

Figures

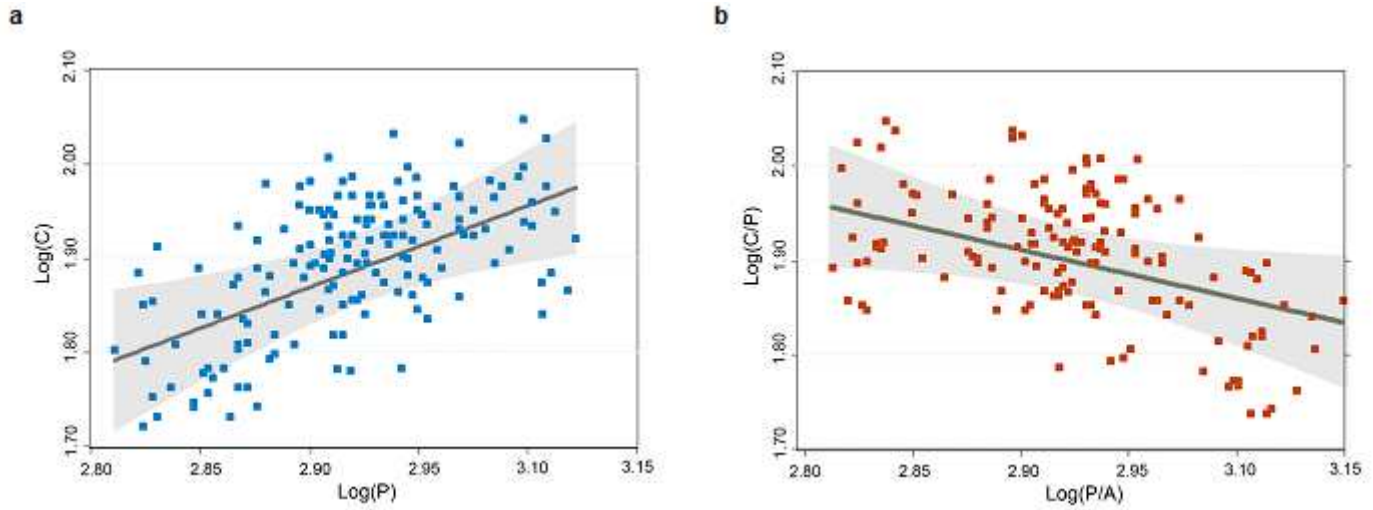


Figure 1

See the Manuscript Files section for the complete figure caption.

a Sample cities

b Summer UHI / Winter UHI

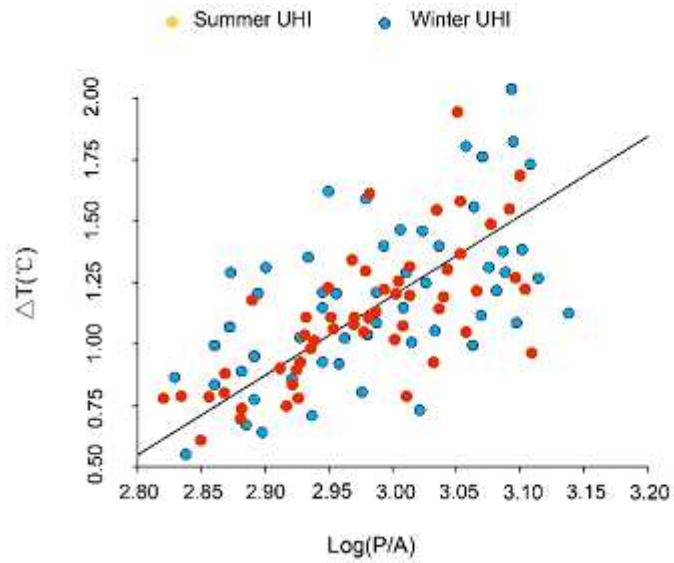
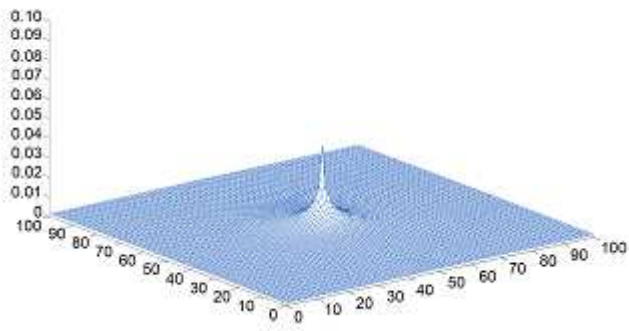


Figure 2

See the Manuscript Files section for the complete figure caption.

a Low-risk constraint



b High-risk constraint

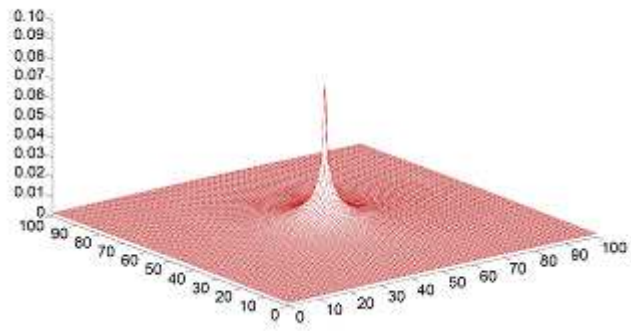
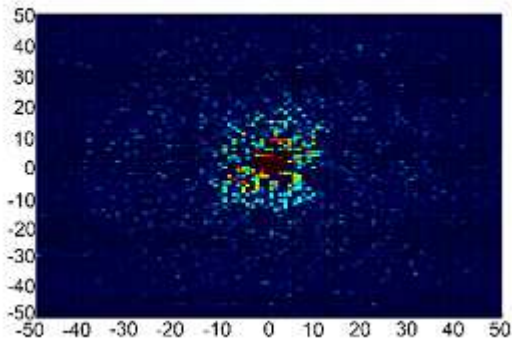


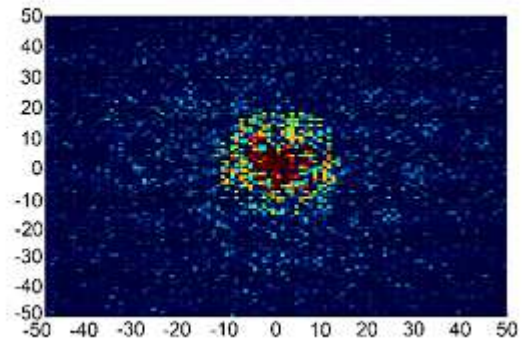
Figure 3

See the Manuscript Files section for the complete figure caption.

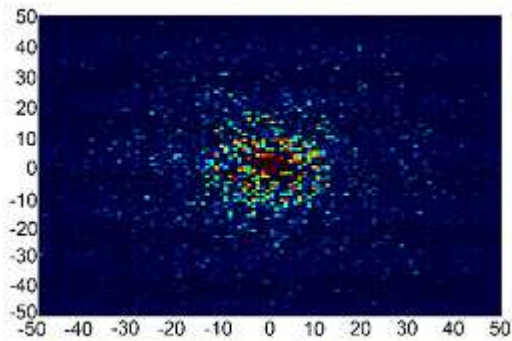
a $g = 0.2, \delta = 2.5$



c $g = 0.2, \delta = 2.5$



b $g = 0.7, \delta = 1.5$



d $g = 0.7, \delta = 1.5$

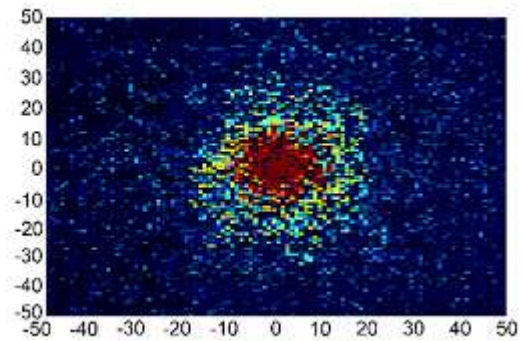


Figure 4

See the Manuscript Files section for the complete figure caption.

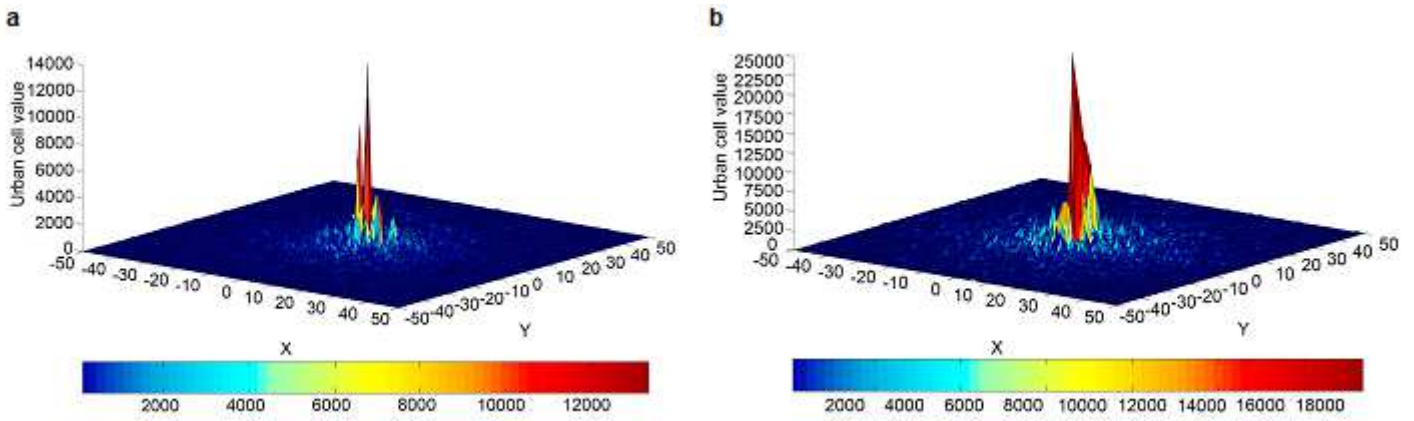


Figure 5

See the Manuscript Files section for the complete figure caption.

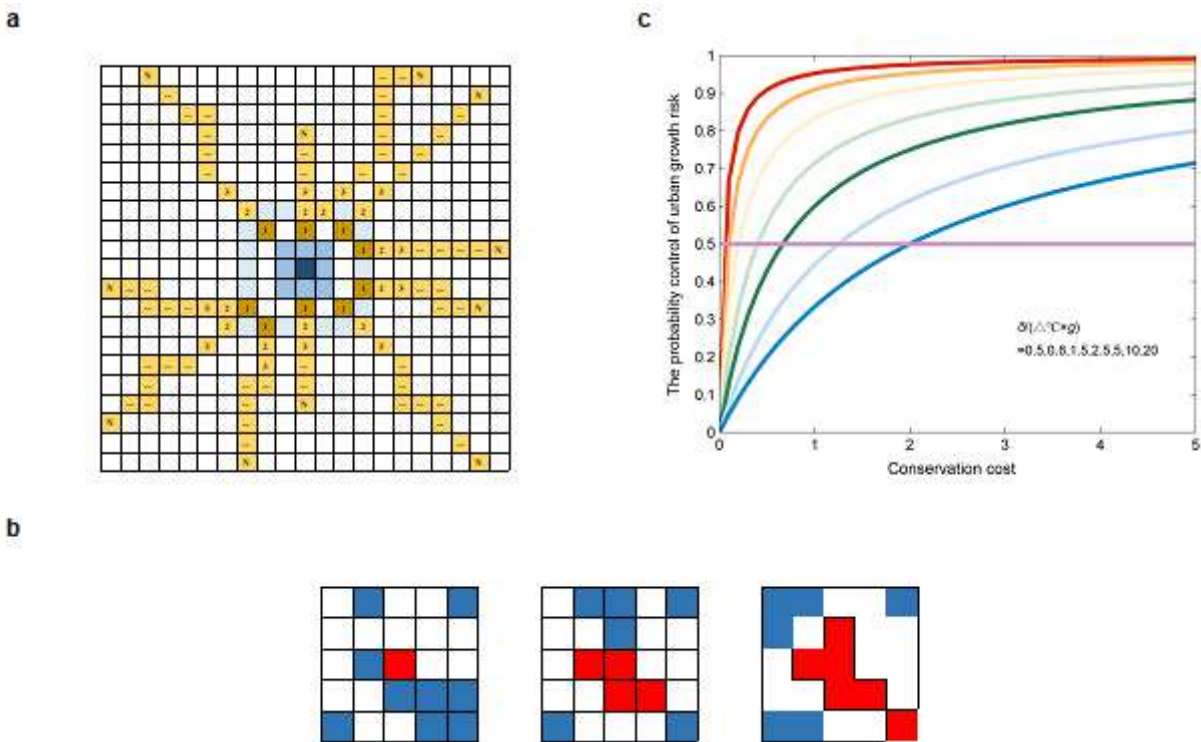


Figure 6

See the Manuscript Files section for the complete figure caption.

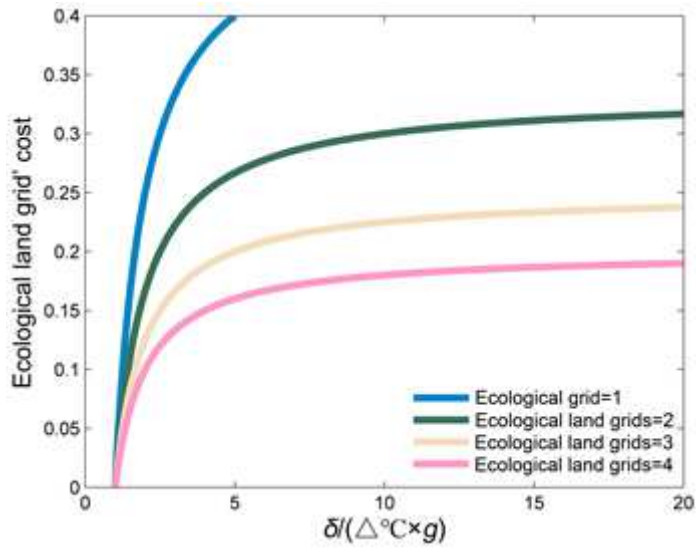


Figure 7

See the Manuscript Files section for the complete figure caption.

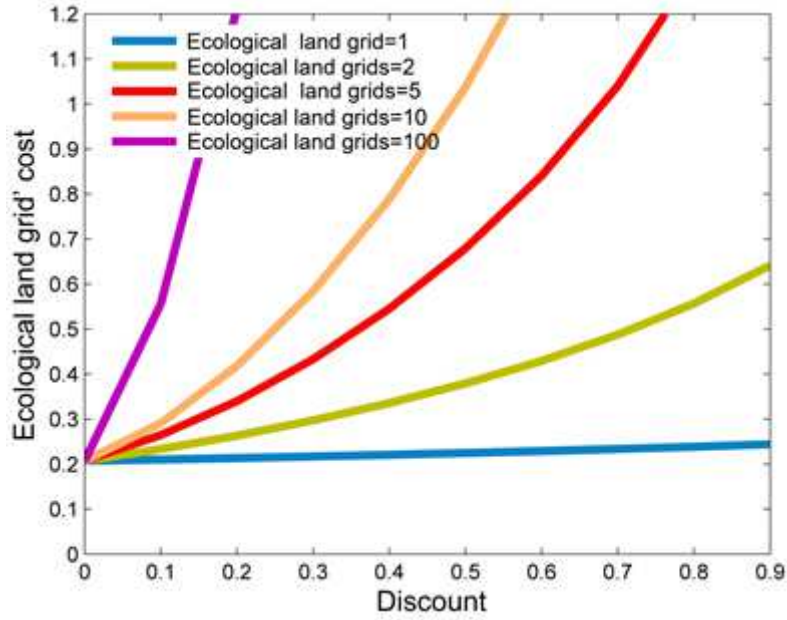


Figure 8

See the Manuscript Files section for the complete figure caption.

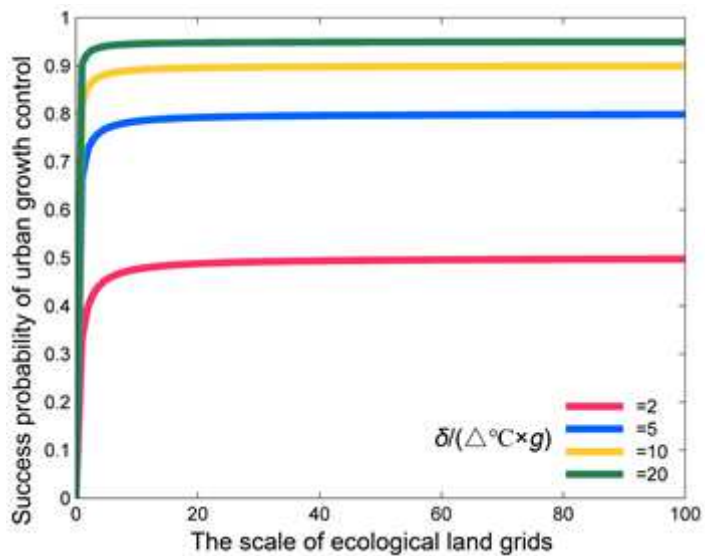


Figure 9

See the Manuscript Files section for the complete figure caption.

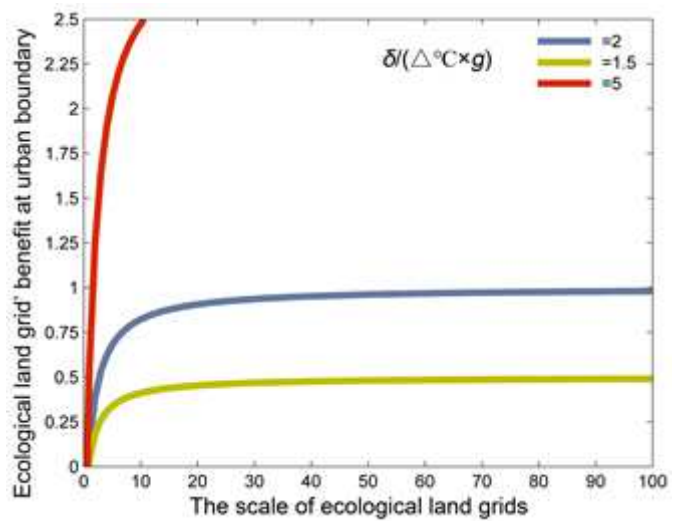


Figure 10

See the Manuscript Files section for the complete figure caption.

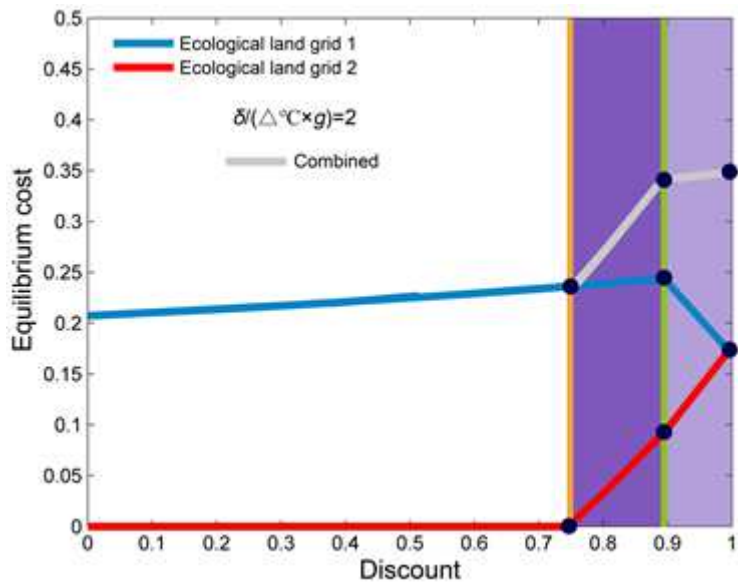


Figure 11

See the Manuscript Files section for the complete figure caption.

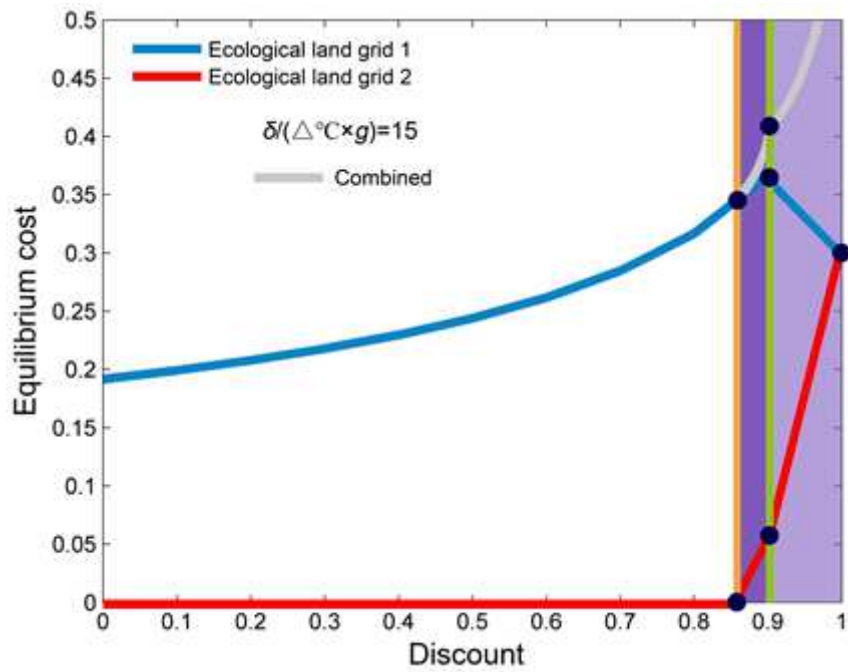


Figure 12

See the Manuscript Files section for the complete figure caption.

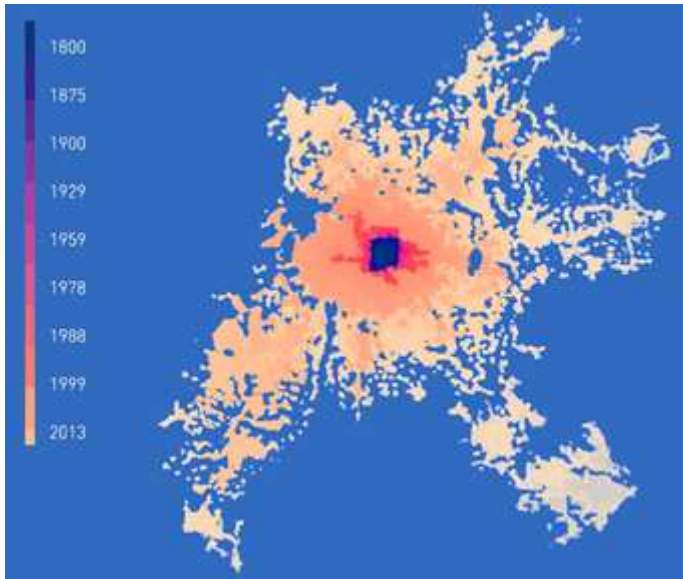


Figure 13

See the Manuscript Files section for the complete figure caption.